

2 Recent Development in IR Sensor Technology 3 for Monitoring Subsea Methane Discharge

4 AUTHORS

5 Mark Schmidt

6 Peter Linke

7 GEOMAR Helmholtz Centre for
8 Ocean Research Kiel, Kiel, Germany

9 Daniel Esser

10 CONTROS Systems & Solutions
11 GmbH, Kiel, Germany

12 Introduction

13 Natural marine hydrocarbon seeps
14 are important sources of methane
15 (CH₄) to the surface sediments, the
16 benthic boundary layer, and eventually
17 to the water column and atmosphere.
18 CH₄ is a potent greenhouse gas that
19 warms the Earth about 23 times more
20 than carbon dioxide (CO₂) when aver-
21 aged over 100 years. Quantifying the
22 discharge of CH₄ from the seabed,
23 its fate in the water column and its
24 flux to the atmosphere has been the
25 subject of ongoing research on many
26 different fronts (e.g., Clark et al.,
27 2000; McGinnis et al., 2006; Judd
28 & Hovland, 2007; Westbrook et al.,
29 2009; Faure et al., 2010). Furthermore,
30 a natural subsea hydrocarbon seep can
31 serve as an ideal analogon for studying
32 gas leakage scenarios from subsea con-
33 structions like gas/oil transport lines,
34 active or abandoned wellheads, etc.
35 (Leifer et al., 2006). Moreover, the dis-
36 solution behavior and transport of gas
37 in the water column at variable ocean-
38 ographic conditions, like currents,
39 horizontal/vertical eddies, tidal changes,
40 or stratified water columns can be stud-
41 ied at natural seepage sites (e.g., Leifer
42 et al., 2006; McGinnis et al., 2006,

43 ABSTRACT

44 Recently developed methane sensors, based on infrared (IR) absorption tech-
45 nology, were successfully utilized for subsea methane release measurements.
46 Long-term investigation of methane emissions (fluid flux determination) from nat-
47 ural methane seeps in the Hikurangi Margin offshore New Zealand were performed
48 by using seafloor lander technology. Small centimeter-sized seep areas could be
49 sampled at the seafloor by video-guided lander deployment. *In situ* sensor mea-
50 surements of dissolved methane in seawater could be correlated with methane con-
51 centrations measured in discrete water samples after lander recovery. High
52 backscatter flares determined by lander-based Acoustic Doppler Current Profiler
53 (ADCP) measurement indicate bubble release from the seafloor. Highest methane
54 concentrations determined by the IR sensor coincided with periods of high ADCP
55 backscatter signals. The high fluid release cannot be correlated with tidal changes
56 only. However, this correlation is possible with variability in spatial bubble release,
57 sudden outbursts, and tidal changes in more quiescent seepage phases.

58 A recently developed IR sensor (2,000 m depth-rated) with a detection limit for
59 methane of about 1 ppm showed good linearity in the tested concentration range
60 and an acceptable equilibration time of 10 min. The sensor was successfully oper-
61 ated offshore Santa Barbara by a small work-class ROV at a natural methane seep
62 (Farrar Seep). High background methane concentration of 50 nmol L⁻¹ was
63 observed in the coastal water, which increases up to 560 nmol L⁻¹ in dissolved
64 methane plumes south of the seepage area. ROV- and lander-based sensor deploy-
65 ments have proven the applicability of IR sensor technology for the determination
66 of subsea methane release rates and plume distribution. The wide concentration
67 range, low detection limit, and its robust detection unit enable this technology
68 for both subsea leak detection and oceanographic trace gas investigations.

69 **Keywords:** methane, sensor development, natural hydrocarbon seeps, subsea leak
detection

70 2011; Schneider von Deimling et al.,
71 2010). Here, we report on the devel-
72 opment and deployment of novel
73 methane sensors, based on infrared
74 absorption technology, which were
75 tested in two different subsea settings.
76 The first setting was a long-term mul-
77 tisensor deployment with a benthic
78 lander, which was placed for 41 h at
79 a 670-m-deep CH₄ cold-seep at the
80 seafloor in the Hikurangi Margin,

81 New Zealand. The second one was a
82 shallow water test of ROV-operated
83 sensor measurement at a natural hydro-
84 carbon seep offshore Santa Barbara,
85 California.

86 CH₄ Sensor Deployment 87 on a Deep Sea Lander

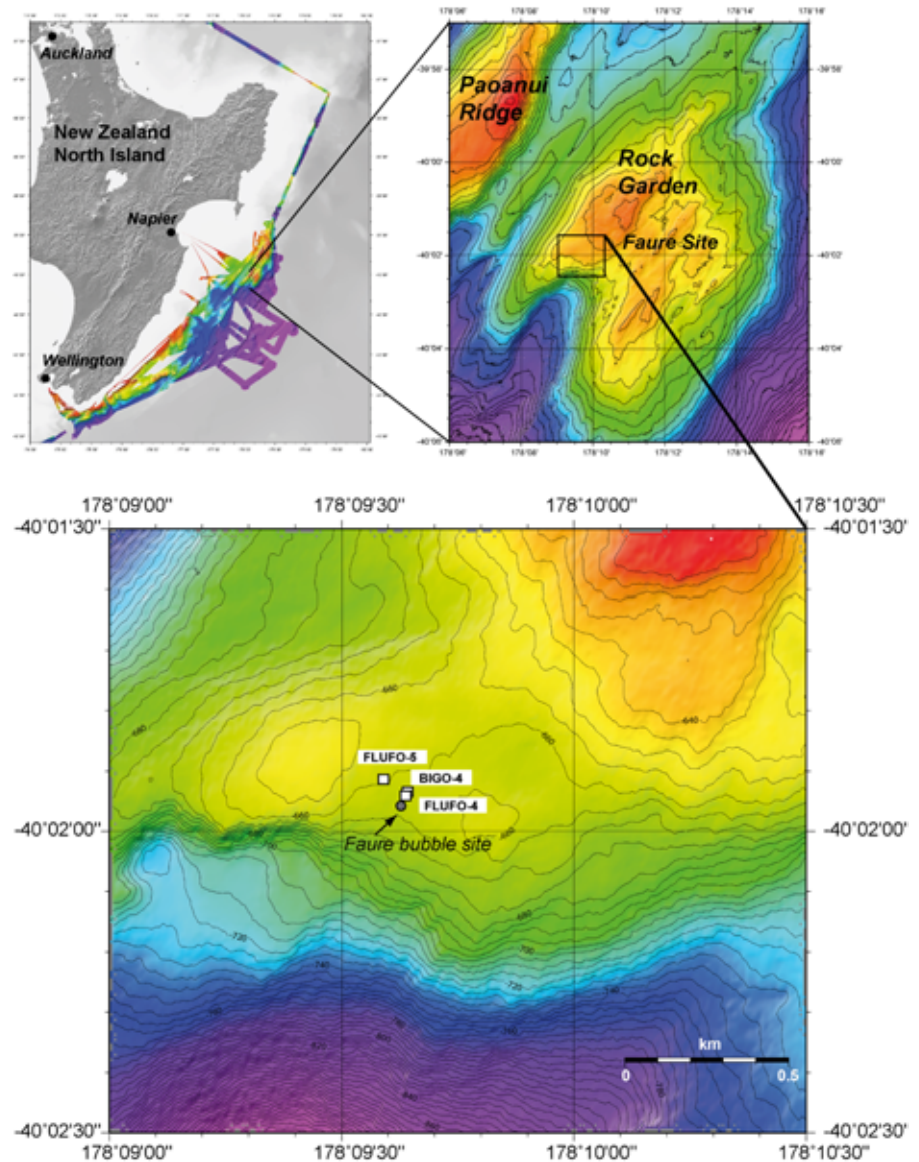
88 A novel methane sensor HydroC™
89 of CONTROS System & Solutions

90 GmbH, Germany, was deployed on
 91 a benthic lander equipped with a
 92 wide range of instrumentation to
 93 study the role of physical parameters
 94 on exchange processes in the benthic
 95 boundary layer. Benthic landers provide
 96 a stationary study platform decoupled
 97 from the movement of the ship and
 98 simultaneously measure several physical,
 99 chemical, and biological parameters
 100 across the sediment water interface. The
 101 Fluid Flux Observatory (FLUFO) was
 102 deployed for *in situ* flux measurements
 103 of methane and oxygen in about 670-m
 104 water depth at a methane seep setting
 105 known as Rock Garden by local fishermen
 106 (Figure 1). This area is situated at the
 107 southern termination of Ritchie Ridge and
 108 is uplifted by the subduction of a
 109 seamount beneath the outer Hikurangi
 110 Margin at the east coast of New Zealand's
 111 North Island. Townend (1997) estimated
 112 that more than 20 m³ of fluids are being
 113 squeezed from accreted and subducted
 114 sediments along each meter of the
 115 Hikurangi Margin every year, which
 116 results in abundant evidence of escaping
 117 gas offshore (Faure et al., 2010; Linke
 118 et al., 2010; Naudts et al., 2010) and
 119 onshore (Campbell et al., 2008). The
 120 deployment was part of a large campaign
 121 involving a large range of equipment
 122 and scientific disciplines to study the
 123 methane seeps at the Hikurangi Margin
 124 (Greinert et al., 2010).

126 The observatory consists of a titanium
 127 tripod frame that carries 21 Benthos
 128 glass spheres for buoyancy and ballast
 129 weights attached to each leg (Figure 2a).
 130 The release of the ballast weights is
 131 controlled by two acoustic releasers.
 132 FLUFO is equipped with two circular
 133 benthic chambers, each covering a
 134 sediment area of 651.4 cm². A video-
 135 guided launching system (LAUNCHER)
 136 allowed smooth placement of the
 137 observatory on a

FIGURE 1

Overview map showing the bathymetry of the Hikurangi Margin at the east coast of New Zealand, mapped during R/V SONNE cruise SO191 in 2007 (modified from Linke et al., 2010). The enlarged bathymetric maps depict the Rock Garden area with stations relevant for this paper; for example, the site of vigorous gas discharge (Faure bubble site) discovered during a ROV dive (Naudts et al., 2010) and two other lander stations (FLUFO-4 and BIGO-4) described in Linke et al. (2010).

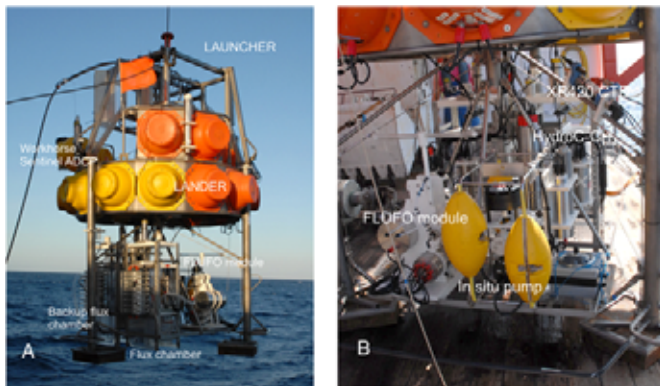


138 selected site at the seafloor (Pfnankuche
 139 & Linke, 2003). Two to three hours
 140 after deployment, the benthic flux
 141 chambers were slowly driven into the
 142 sediment. Seabed methane emission
 143 was monitored with eight sequentially
 144 water samples taken from each cham-
 145 ber by means of glass syringe sam-
 146 plers. Sampling (monitoring) periods

147 were about 34 (FLUFO-5) and 40 h
 148 (FLUFO-4, BIGO-4), respectively.
 149 After the *in situ* incubation, the bot-
 150 tom of the chambers was closed with
 151 a shutter to recover the sediments for
 152 further analyses. After recovery, syringe
 153 water samples retrieved during lander
 154 deployment were immediately trans-
 155 ferred into the cold room, where

FIGURE 2

Launch of the Fluid Flux Observatory (FLUFO) with the video-guided launcher on top showing the different scientific modules integrated in the back (a) and in the front (b) of the lander (modified from Linke et al., 2010).



subsamples were obtained for the determination of oxygen and methane (Linke et al., 2010).

Next to the chambers, the lander carried the HydroCTM methane sensor for *in situ* measurements up to 4,000 m water depths (Figure 2b). The high-pressure seawater side is separated by a permeable membrane from the internal infrared detection unit. An internal pump system increases equilibration of internal partial pressure of, for example, methane with the dissolved methane in seawater. Concentrations of methane were determined by using optical NDIR absorption technique. Large quantities of methane accumulated in the internal gas circuit can actively be removed with a patented exhaust system. The sensor was calibrated to detect CH₄ concentrations as low as approximately 100 nmol L⁻¹, and data were logged by a 24-bit SmartDI controller.

The HydroCTM methane sensor was mounted upright at the lander frame to avoid any trapping of gas bubbles in front of the membrane inlet. Beside the methane sensor, FLUFO was equipped with an upward-looking Acoustic Doppler Current Profiler

(ADCP; 300 kHz Workhorse Sentinel ADCP, Teledyne RD Instruments, USA) and a small stand-alone memory CTD (Conductivity, Temperature, Depth; XR420, RBR Ltd., Ottawa, Canada). The CTD was also equipped with an optical backscatter sensor (SeaPoint), which measures light scattered by particles suspended in water.

The lander was deployed in the vicinity of a methane gas vent named Faure bubble site (FLUFO-5; Figure 2). Here, bubble release occurs from differently sized depressions, which are often aligned in NW-SE direction; the largest depression observed by a ROV was 50 cm in diameter and 15 cm deep (Naudts et al., 2010). These observations clearly showed that the depressions are formed by the often violent release of bubbles. Naudts and coworkers observed that the bubbles entrained sediment particles, which then get carried away by the water currents, creating the depressions and a sediment outfall away from the venting hole. The data obtained with the HydroCTM sensor depict pulses of CH₄ emission (Figure 3a), ranging between 150 and 200 nmol L⁻¹. Water samples obtained from the ambient bottom water during

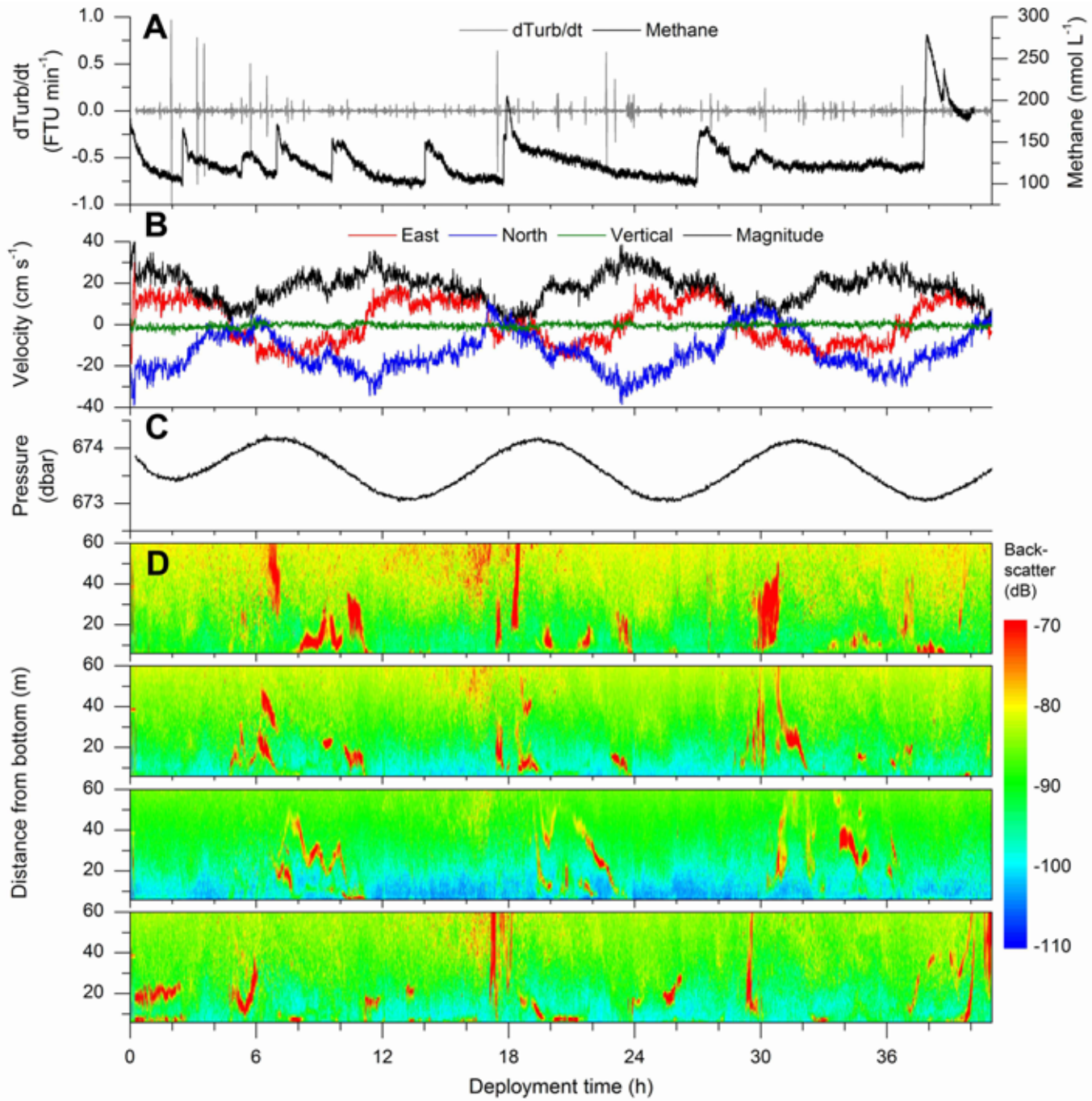
a parallel deployment of another lander (BIGO-4; Figure 2) at the same height above the sediment water interface like the sensor showed two distinct peaks with CH₄ concentrations of 189 and 190 nmol L⁻¹, respectively (Linke et al., 2010), which are in the same range of the measurements obtained with the HydroCTM sensor. On the other hand, the data shown here depict that the sensor needed some time of relaxation after it had experienced high a peak of CH₄ before it was able to record another sudden increase.

However, the pulses seen in the HydroCTM sensor data correspond with increases in the backscatter strength detected in all four beams of the upward-looking ADCP (Figure 3d). The “flares” (presumed to be bubbles) persisted for 10–60 min, and some of them covered almost the whole acoustic depth range (100 m) of the ADCP. No associated signal was observed in the turbidity data obtained from the CTD (Figure 3a). The occurrence of the flares does not seem to be related to a sudden or tidal hydrostatic pressure drop (Figure 3c). In fact, some of the outburst occurred during high tide and at maximum current velocities of more than 20 cm s⁻¹ (Figure 3b). This is in agreement with results of Linke et al. (2010) from another lander deployment next to the Faure Site (FLUFO-4; Figure 2). They found CH₄ concentration fluctuations in both the ambient bottom water and the chamber water, which coincided with tidally induced fluctuations of currents and acoustic backscatter flares in the ADCP record.

Furthermore, these measurements agree very well with ROV observations in the area reporting highly variable spatial bubble release rates and bubble sizes, with periods of low activity, alternating with periods of violent outbursts (Naudts et al., 2010).

FIGURE 3

Physical measurements obtained simultaneously to the changes in CH₄ concentration during deployment of FLUFO-5. Top to bottom: (a) turbidity changes and CH₄ concentration, (b) depth-averaged velocity time series, (c) local hydrostatic pressure, and (d) ADCP backscatter (all four beams).



266
267
268
269
270

High-Sensitive Methane Sensor (HISEM) Development

A new methane sensor, which should fulfill the needs for scientific

271 trace gas (i.e., CH₄) investigations in
272 the oceans and for subsea leak detec-
273 tion, is currently under development
274 (www.martec-era.net). The sensor
275 technology is based on laser diode IR
276 absorption technology that provides

277 excellent detection limits at good
278 signal-to-noise ratios. The actual
279 configuration is a 2,000-m depth-rated
280 version with a (Contros HydroC™)
281 membrane-inlet configuration. The
282 system was tested in the laboratory

277
278
279
280
281
282

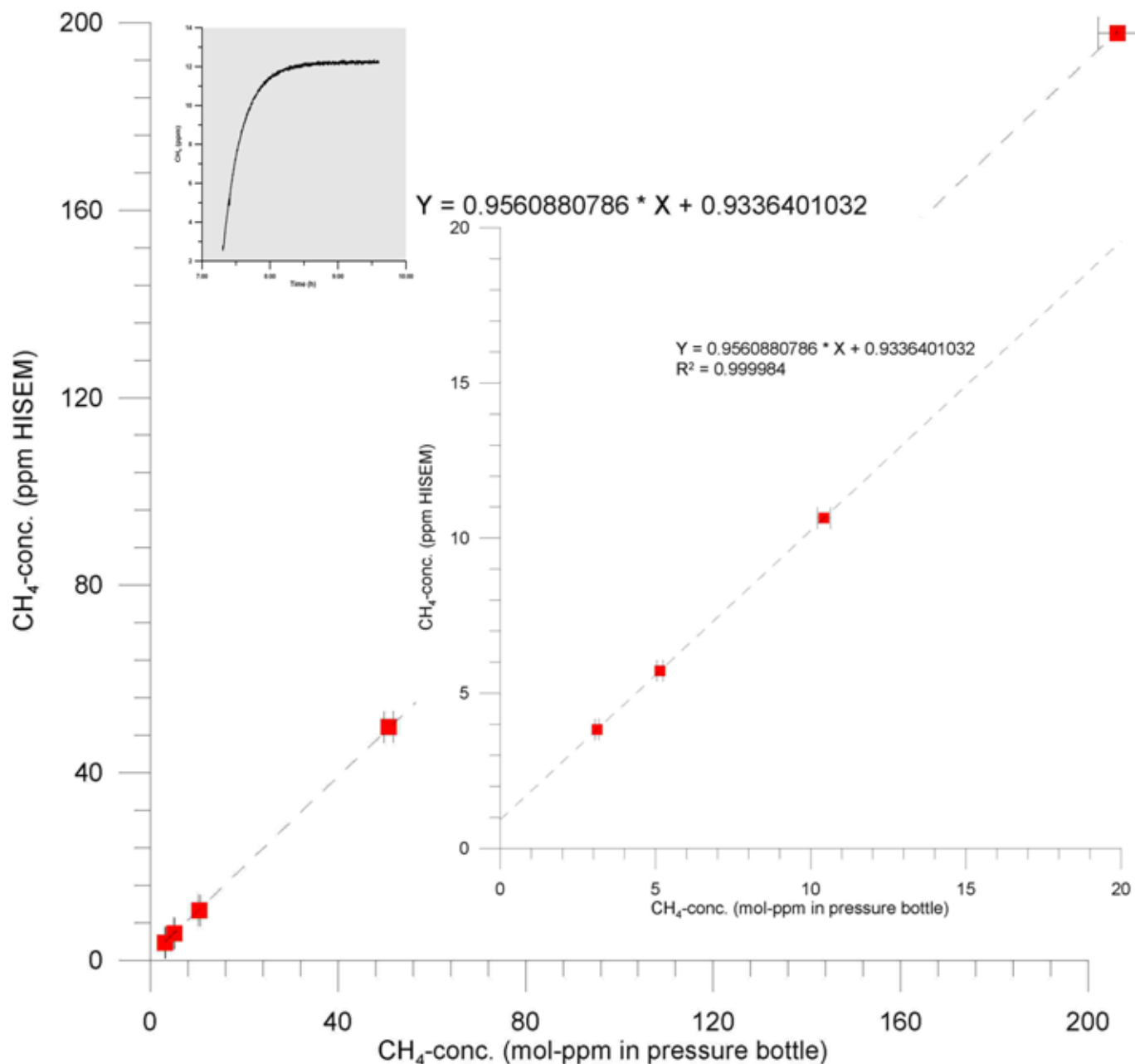
283 against various partial pressures of 291 Gas exchange with atmosphere is pre-
 284 methane dissolved in water in a tem- 292 vented in the semiclosed system. The
 285 perature controlled (4–15°C) water- 293 response of the sensor signal is con-
 286 filled calibration tube. The water 294 tinuously recorded during testing, and
 287 is continuously equilibrated at atmo- 295 equilibration of the signal is established
 288 spheric pressure with standard gas mix- 296 with a response time (t_{65}) of about
 289 tures of methane (3–200 mol-ppm) in 297 10 min after partial methane pressures
 290 synthetic air pressure bottles (~200 bar). 298 have been changed in the tube (Figure 4).

299 The detection limit of the HISEM of 300
 301 about 1 ppm could be determined with
 302 a signal-to-noise ratio of 5. 303

304 The sensor output (ppm unit) shows
 305 good linearity ($R^2 = 0.99998$) against
 306 the known pressure bottle concentra-
 307 tions given in mol-ppm with an offset
 308 of ~1 ppm (Figure 4). The correlation

FIGURE 4

Methane concentrations determined with the HISEM system, which was placed in a water-filled calibration tube at 4°C. The water is equilibrated with methane by using different gas mixtures (3, 5, 11, 50, 100, and 200 mol-ppm CH₄ in pressure bottles).



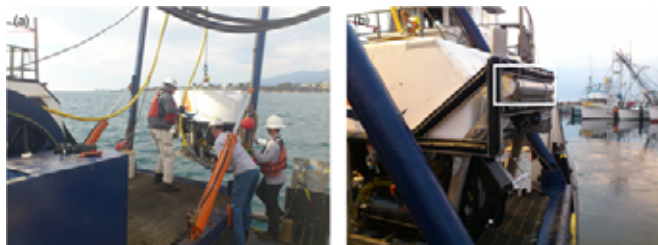
307 was confirmed by parallel determina-
308 tion of dissolved methane concentra-
309 tions sampled from the calibration
310 tube. These methane analyses were
311 conducted by using head space sam-
312 pling technique and subsequent gas
313 chromatographic analysis.

314 HISEM Offshore Test Site

315 To test the sensor performance
316 for methane plume detection and its
317 offshore practicability in operating
318 the system with a small work-class re-
319 motely operated vehicle (i.e., HYSUB
320 20 ROV), a 3-day offshore campaign
321 was performed in November 2012
322 near Santa Barbara, Southern Califor-
323 nia. The offshore test site that was cho-
324 sen is named *Farrar Seep* and is located
325 within the Coal Oil Point seep area in
326 the inner Santa Barbara Channel (Fig-
327 ure 5a) about 1,300 m east of the Uni-
328 versity of California, Santa Barbara
329 area (Figure 5b). The Farrar Seep is a
330 natural hydrocarbon seep that is indi-
331 cated by gas bubble release from the
332 seafloor at about 22 mbsl. Natural
333 gas seeps in the area of the inner
334 Santa Barbara Channel can be charac-

FIGURE 6

(a) Deployment of the \$2ROV from the starboard site of M/V *Danny C.* (b) The HISEM prototype (marked by white rectangle) was mounted behind the bumper bar of the ROV.

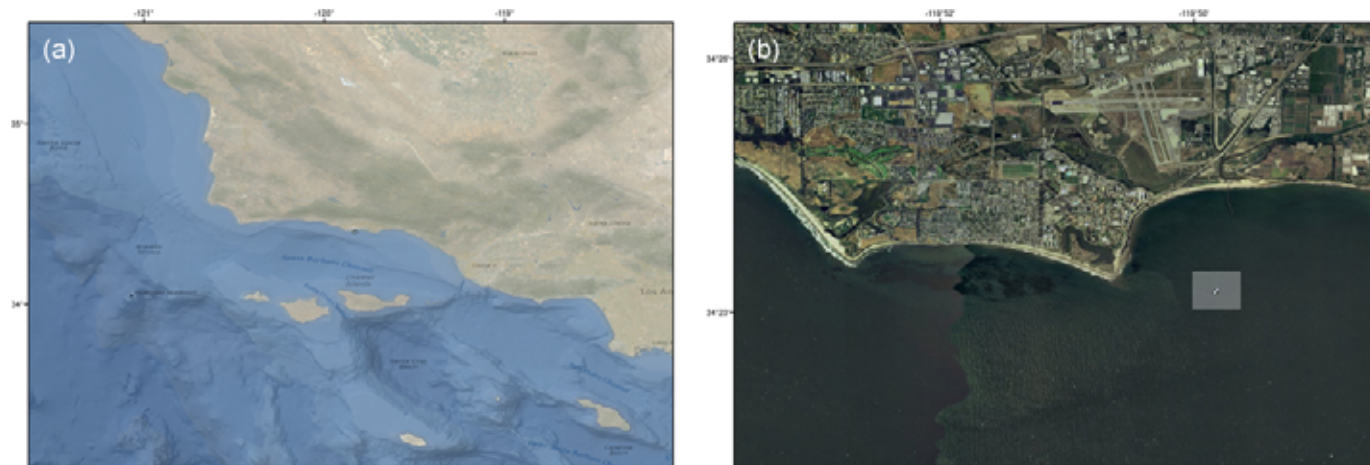


335 terized by low seepage activity, and the
336 gas composition of bubbles emanating
337 from the seafloor consists of up to 90%
338 of methane and 10% of higher hydro-
339 carbons (e.g., Leifer et al., 2006). As
340 gas bubbles dissolve and exchange
341 their gas content during uplift in seawa-
342 ter, dissolved gas plumes are formed in
343 the water column and the initial hydro-
344 carbon content of the bubbles decreases
345 (e.g., Leifer & Patro, 2002; Clark et al.,
346 2003; McGinnis et al., 2006). Numer-
347 ous natural gas and oil seeps exist in the
348 inner Santa Barbara channel, which
349 lead to general high background con-
350 centrations of dissolved methane in
351 the area (e.g., ~20–100 nmol L⁻¹;
352 Clark et al., 2000).

353 To measure dissolved methane
354 concentrations during ROV dives, the
355 HISEM system was mounted parallel
356 behind the upper bumper bar of the
357 HYSUB 20 (Figure 6). The head (mem-
358 brane inlet) of the HISEM prototype
359 was connected with a plastic tube to a
360 suction inlet at the front of the ROV. A
361 metal filter was mounted to the suction
362 inlet, and the inlet area was monitored
363 permanently by cameras. A second
364 tube connected the suction inlet by a
365 y-adapter with a CTD and a commer-
366 cial leak detection device (Combination
367 of HydroC-CH₄, Fluorometer). A
368 constant water flow through the tubing
369 was guaranteed by two Seabird pumps,
370 which operated inline the tubes.

FIGURE 5

(a) Map of the overall area of the Santa Barbara channel in Southern California. The test site is marked as a small open circle. (b) Farrar Seep offshore test site (shaded rectangle), about 1,300 m east of the University of California Santa Barbara area.



ROV-Based Sensor Measurements

Two N-S and four W-E ROV dives were conducted at the 28th and 29th of November 2012 at the estimated location of the Farrar Seep (Figure 5b). The average length of a ROV dive track was about 250 m. Furthermore, one vertical dive track was conducted at the estimated center of the seep (Figure 5b). During all dives, water depth, temperature, conductivity (SV48 CTD, Sea and Sun Technology) and methane sensor data (HISEM) were recorded continuously. However, the ROV stopped every 15 m for 1–2 min to increase the total measuring time. The homogeneous temperatures of about 15.8°C and salinities of about 33.4 PSU measured during the ROV dives indicate a well-mixed water column in this coastal area during November 2012. The water depth of the test area is about 16–30 mbsl and ROV dive tracks plotted in Figure 7 were performed above seafloor at elevations of 2 and 12 m, respectively. Due to strong currents in the area and especially a current direction and current speed change between the 28th and 29th of November 2012 (Goleta Point buoy data, SCCOOS.org), navigating the ROV was challenging and deviations from predefined track lines were about 15 m. The Farrar Seep location could be verified at 119°49.836'W and 34°24.157'N (WGS84) by measuring a CH₄ concentration maximum (up to 260 ppm and 334 nmol L⁻¹, respectively) while crossing the central seepage site with the ROV at 2 m elevation above seafloor (Figure 8). The minimum concentration of dissolved methane, which was determined in water masses in the test area, was ~50 nmol L⁻¹.

The center of the main seepage activity of the Farrar Seep was also

FIGURE 7

ROV dive tracks conducted in the test area “Farrar Seep.”

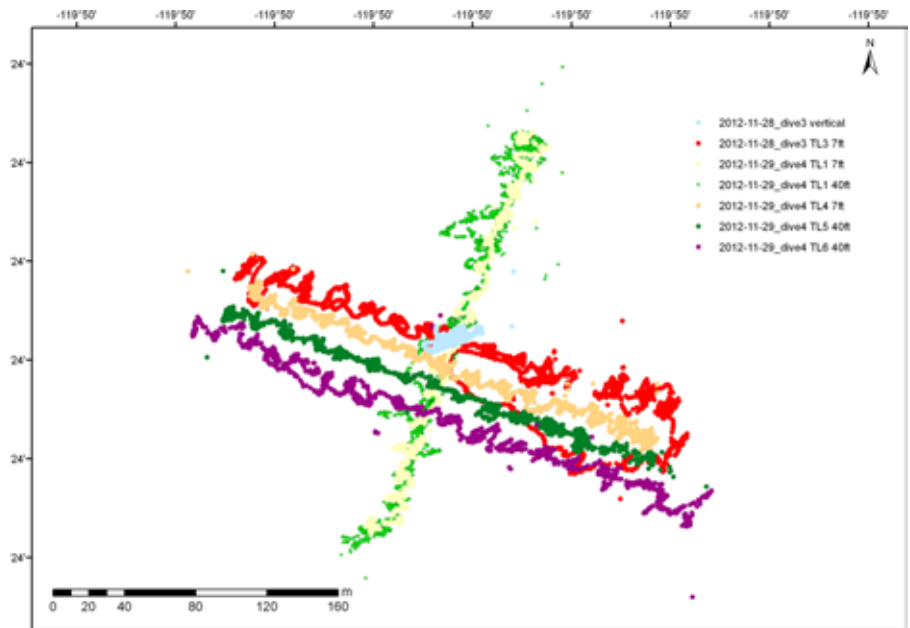


FIGURE 8

Methane sensor signal recorded with HISEM about 2 m above the seafloor during ROV track line 1 at the 28th and 29th of November 2012. Track line 1 is the N-S profile and crosses the Farrar Seep (Figure 3).

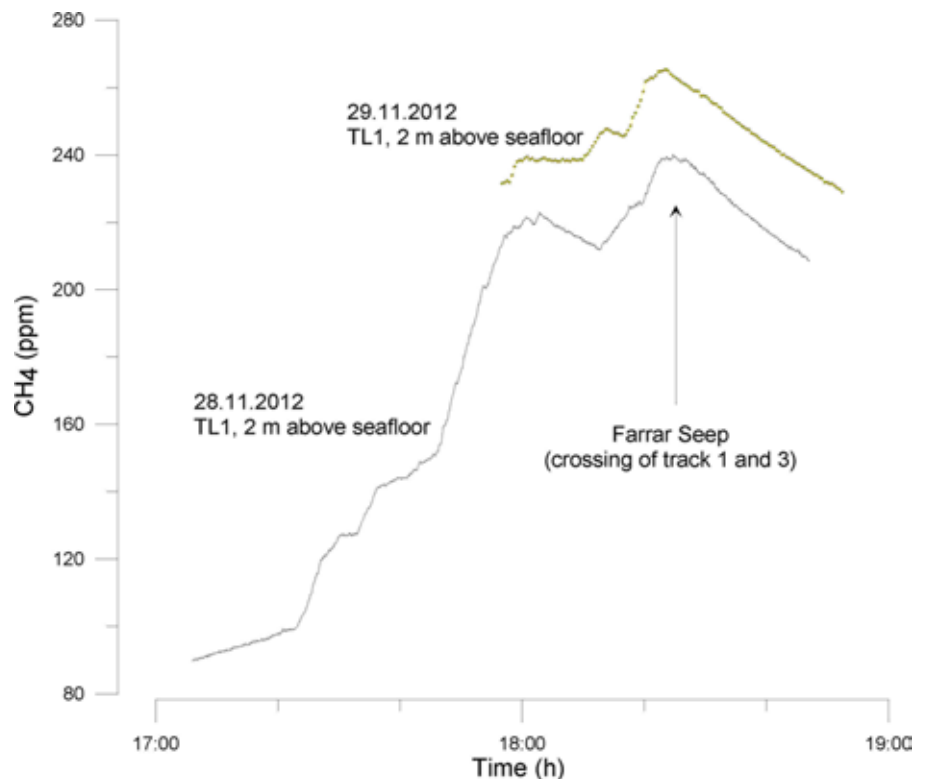
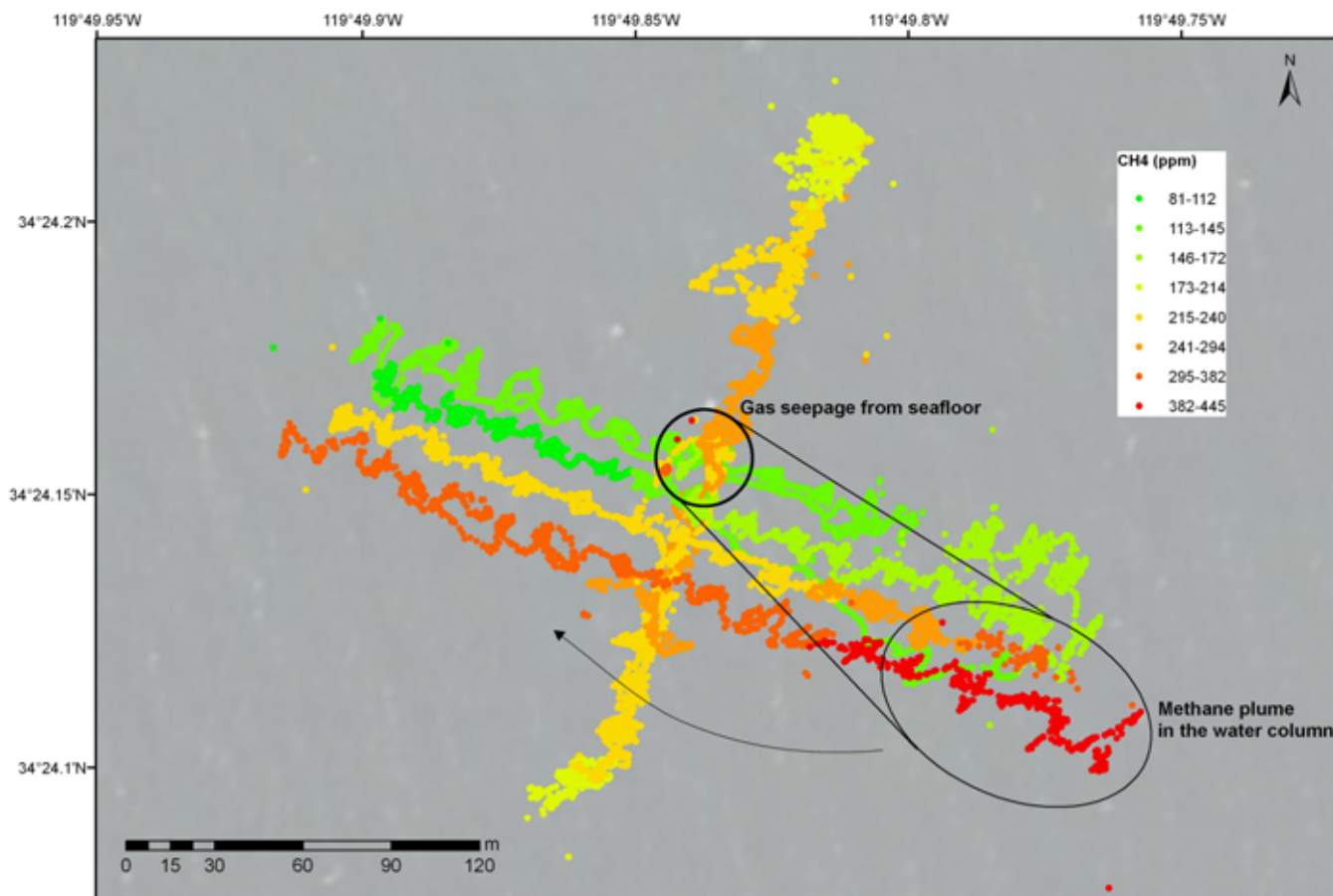


FIGURE 9

Spatial methane concentrations at Farrar Seep measured by HISEM during ROV dives. The concentration of methane is given in ppm. The total range measured by HISEM corresponds to dissolved methane concentrations of 50–560 nmol L⁻¹ in the test area.



419 indicated by the ship's echo-sounder
420 (acoustic blankening by gas bubbles)
421 and ground-truthing by ROV (video
422 observations). Note that measuring
423 the dissolved gas content within the
424 bubble streams emanating from the
425 seafloor did not increase the HISEM
426 sensor concentration signal. The con-
427 centration pattern of November 28th
428 could be verified by following the same
429 track on the 29th (Figure 8). The devi-
430 ation of methane concentration data of
431 about 25 nmol L⁻¹ measured within
432 the central seep area is possibly related
433 to a weakening of the local current re-
434 gime on the 29th (<http://sccoos.org/>).

435 The dimensions of the main (dis-
436 solved) methane plume were about

437 50–150 m around the seepage site
438 (Figure 9). However, dissolved gas
439 plumes with high methane concentra-
440 tions (up to 560 nmol L⁻¹) were also
441 examined towards the east and south
442 at about 12 m above the seafloor (Fig-
443 ure 9). In general, the dissolved meth-
444 ane concentrations are highest towards
445 the south, which could indicate a pre-
446 ferred rotation of the methane plume
447 direction from east to south and then
448 west (Figure 9).

449 Conclusions

450 Subsea determination of dissolved
451 methane concentration can be con-
452 ducted by using infrared absorption

453 technology. The technology, mea-
454 suring the partial pressure of methane
455 in a separated gas chamber, is com-
456 bined with a membrane inlet, which
457 separates high-pressure conditions
458 of the deep sea from the gas chamber
459 at normal pressure. Recent advances
460 in laser diode technology led also
461 to cost-effective and high-sensitive
462 infrared absorption units. The newly
463 designed high-sensitive methane sen-
464 sor (HISEM), which combines laser
465 diode infrared absorption with mem-
466 brane inlet technology, closes a gap
467 between the needs of small and less
468 sensitive methane sniffers used for
469 offshore leak detection (Oil & Gas
470 Industry) and oceanographic trace gas

471 determinations down to 1–2 nmol L⁻¹
472 of CH₄ (equilibrium concentration of
473 seawater with the atmosphere).

474 Membrane-inlet IR absorption
475 sensors can be used for long-term
476 measurements at the seafloor (e.g.,
477 lander-based deployment). The de-
478 termination of, for example, varying
479 methane concentrations in the vicinity
480 of a methane seep have to be combined
481 with determination of temperature,
482 salinity, and pressure variations, as
483 well with current measurements (i.e.,
484 using ADCPs). This combination is
485 the basic information used to deter-
486 mine (dissolved) gas fluxes from natu-
487 ral seeps or leaking constructions at
488 the seafloor.

489 Focused release of methane from
490 subsea seeps and of rising plumes of
491 dissolved methane can be monitored
492 with ROV-based IR sensor technol-
493 ogy. However, the quantification of
494 methane release also needs some basic
495 oceanographic information about the
496 local current regime and physical
497 parameters (T, S, P) along the ROV
498 dive tracks. This could be realized dur-
499 ing onboard CTD measurements and
500 an upward-looking ADCP deployed
501 at the seafloor. A miniaturization of
502 the recently developed high sensitive
503 methane sensor (HISEM) is prere-
504 quisite to use this technology onboard
505 inspection class ROVs.

506 Acknowledgments

507 The HISEM system development
508 is funded by the German Ministry
509 BMWi (Project No. 03SX301) within
510 the European funding initiative
511 MARTECH (ERA-NET, Maritime
512 Technologies). Wintershall Noordzee
513 is kindly acknowledged for support-
514 ing the offshore operations and ROV
515 adaptions.

516 Corresponding Author:

517 Mark Schmidt
518 GEOMAR Helmholtz Centre for
519 Ocean Research Kiel
520 Wischhofstr. 1-3,
521 24148 Kiel, Germany
522 Email: mschmidt@geomar.de

523 References

- 524 **Campbell**, K.A., Francis, D.A., Collins, M.,
525 Gregory, M.R., Nelson, C.S., Greinert, J.,
526 & Aharon, P. 2008. Hydrocarbon seep-
527 carbonates of a Miocene forearc (East Coast
528 Basin), North Island, New Zealand. *Sediment*
529 *Geol.* 204:83-105. [http://dx.doi.org/10.1016/](http://dx.doi.org/10.1016/j.sedgeo.2008.01.002)
530 [j.sedgeo.2008.01.002](http://dx.doi.org/10.1016/j.sedgeo.2008.01.002).
- 531 **Clark**, J.F., Leifer, I., Washburn, L., &
532 Luyendyk, B.P. 2003. Compositional changes
533 in natural gas bubble plumes; Observations
534 from the Coal Oil Point marine hydrocarbon
535 seep field. *Geo-Mar Lett.* 23:187-93. [http://](http://dx.doi.org/10.1007/s00367-003-0137-y)
536 dx.doi.org/10.1007/s00367-003-0137-y.
- 537 **Clark**, J.F., Washburn, L., Hornafius, J.S., &
538 Luyendyk, B.P. 2000. Dissolved hydro-
539 carbon flux from natural marine seeps to the
540 Southern California Bight. *J Geophys Res.*
541 105(11):509-11,522.
- 542 **Faure**, K., Greinert, J., Schneider von
543 Deimling, McGinnis, D.F., Kipfer, R., &
544 Linke, P. 2010. Methane seepage along
545 the Hikurangi Margin of New Zealand:
546 Geochemical and physical data from the water
547 column, sea surface and atmosphere. *Mar*
548 *Geol.* 272:170-88. [http://dx.doi.org/10.1016/](http://dx.doi.org/10.1016/j.margeo.2010.01.001)
549 [j.margeo.2010.01.001](http://dx.doi.org/10.1016/j.margeo.2010.01.001).
- 550 **Greinert**, J., Lewis, K.B., Bialas, J., Pecher, I.A.,
551 Rowden, A., Bowden, D.A., ... Linke, P.
552 2010. Methane seepage along the Hikurangi
553 Margin, New Zealand: Overview of studies in
554 2006 and 2007 and new evidence from visual,
555 bathymetric and hydroacoustic investigations.
556 *Mar Geol.* 272:6-25. [http://dx.doi.org/](http://dx.doi.org/10.1016/j.margeo.2010.01.017)
557 [10.1016/j.margeo.2010.01.017](http://dx.doi.org/10.1016/j.margeo.2010.01.017).
- 558 **Judd**, A.G., & Hovland, M. 2007. Seabed
559 Fluid Flow: The Impact on Geology, Biology,
560 and the Marine Environment. New York:

Cambridge Univ. Press. 475 pp. <http://dx.doi.org/10.1017/CBO9780511535918>.

Leifer, I., Clark, J., & Luyendyk, B. 2006. Simulation of a Subsurface Oil Spill by a Marine Hydrocarbon Seep. MMS OCS Study 2006-050. Santa Barbara, CA: Coastal Research Center, Marine Science Institute, University of California. MMS Cooperative Agreement Number 14-35-01-00-CA-31063. 81 pp.

Leifer, I., & Patro, R.K. 2002. The bubble mechanism for methane transport from the shallow sea bed to the surface: A review and sensitivity study. *Cont Shelf Res.* 22:2409-28. [http://dx.doi.org/10.1016/S0278-4343\(02\)](http://dx.doi.org/10.1016/S0278-4343(02)00065-1)
00065-1.

Linke, P., Sommer, S., Rovelli, L., & McGinnis, D.F. 2010. Physical limitations of dissolved methane fluxes: The role of bottom-boundary layer processes. *Mar Geol.* 272:209-22. [http://dx.doi.org/10.1016/](http://dx.doi.org/10.1016/j.margeo.2009.03.020)
j.margeo.2009.03.020.

McGinnis, D.F., Greinert, J., Artemov, Y., Beaubien, S.E., & Wuest, A. 2006. Fate of rising methane bubbles in stratified waters: How much methane reaches the atmosphere? *J Geophys Res.* 111:C09007. <http://dx.doi.org/10.1029/2005JC003183>.

McGinnis, D.F., Schmidt, M., DelSontro, T., Themann, S., Rovelli, L., Reitz, A., & Linke, P. 2011. Discovery of a natural CO₂ seep in the German North Sea: Implications for shallow dissolved gas and seep detection. *J Geophys Res (Oceans).* 116:C03013. <http://dx.doi.org/10.1029/2010JC006557>.

Naudts, L., Greinert, J., Poort, J., Belza, J., Vangampelaere, E., Boone, D., ... De Batist, M. 2010. Active venting sites on the gas-hydrate-bearing Hikurangi Margin, Off New Zealand: Diffusive versus bubble-released methane. *Mar Geol.* 272:233-50. <http://dx.doi.org/10.1016/j.margeo.2009.08.002>.

Pfannkuche, O., & Linke, P. 2003. GEOMAR landers as long-term observatories. *Sea Technol.* 44(9):50-5.

Schneider von Deimling, J., Greinert, J., Chapman, N.R., Rabbal, W., & Linke, P. 2010. Acoustic imaging of natural gas seepage

609 in the North Sea: Sensing bubbles controlled
610 by variable currents. *Limnol Oceanogr Meth.*
611 8:155-71. [http://dx.doi.org/10.4319/lom.2010.](http://dx.doi.org/10.4319/lom.2010.8.155)
612 8.155.

613 **Townend**, J. 1997. Subducting a sponge:
614 minimum estimates of the fluid budget of the
615 Hikurangi margin accretionary prism. *Geol*
616 *Soc N Zeal Newsl.* 112:14-6.

617 **Westbrook**, G.K., Thatcher, K.E., Rohling,
618 E.J., Piotrowski, A.M., Pålke, H., Osborne,
619 A.H., ... Aquilina, A. 2009. Escape of methane
620 gas from the seabed along the West Spitsbergen
621 continental margin. *Geophys Res Lett.*
622 36:L15608. [http://dx.doi.org/10.1029/](http://dx.doi.org/10.1029/2009GL039191)
623 2009GL039191.

AUTHOR QUERIES

AUTHOR PLEASE ANSWER QUERIES

Q1: Please check Figure 2 and 3 if labels in image should be lowercase to be consistent with the captions.

Q2: Please provide first name of Schneider von Deimling in Faure et al., 2010 reference.

END OF AUTHOR QUERIES